CSIRO PUBLISHING

Exploration Geophysics, 2012, **43**, 156–161
http://dx.doi.org/10.1071/EG11019

A modified EOM method for *PS*-wave migration

Yun Wang[1] Wei Wang[2,4] Junjie Yin[3]

[1]Institute of Geochemistry, Chinese Academy of Sciences, Guiyang 550002, China.
[2]The State Key Laboratory of Resources and Environmental Information System, Institute of Geographic Sciences and Natural Resources Research, Chinese Academy of Sciences, Beijing 100101, China.
[3]National Engineering Research Center of Coal Bed Methane Ltd., Beijing 100011, China.
[4]Corresponding author. Email: wangweiitpcas@163.com

Abstract. A modified EOM method is developed for *PS*-wave migration based on the equivalent offset migration (EOM) for *P*-waves. This gives better imaging quality than the previous EOM methods by reducing errors from the discretisation of equivalent offsets and suppressing noise from the co-location of source-receiver. An equivalent *PS*-wave velocity is also introduced. Processing real 2-dimensional 3-component seismic data shows that the method can produce a better migrated image than the conventional common conversion point (CCP) method.

Key words: co-location, common conversion point, discretisation, equivalent offset, *PS*-wave.

Received 25 April 2011, accepted 3 April 2012, published online 16 May 2012

Introduction

There are many differences when the nature of converted waves (*PS*-waves) is compared with the nature of *P*-waves (Aki and Richards, 1980). These differences are largely associated with the down-going *P*-wave, the up-going shear waves (*S*-waves) and the asymmetry of the ray-paths. Considering the features of *PS*-wave data, and limits in data acquisition, *PS*-wave analysis often involves issues such as weak reflection energy, and low signal-to-noise ratio (SNR) in common conversion point (CCP) gathers. Sorting and velocity analysis of CCP gathers are affected by inaccuracy in *P*-wave horizon identification, and in velocity picking. These factors influence the SNR and the accuracy of *PS*-wave imaging, thus, it is important to tackle these weaknesses in *PS*-wave imaging.

Following the Huygens–Fresnel model, the *PS*-wave is a specific form of scattered wave in heterogeneous media (Wu and Aki, 1985). When common scatter point (CSP) gathers are obtained under the assumption of equivalent offset (Bancroft

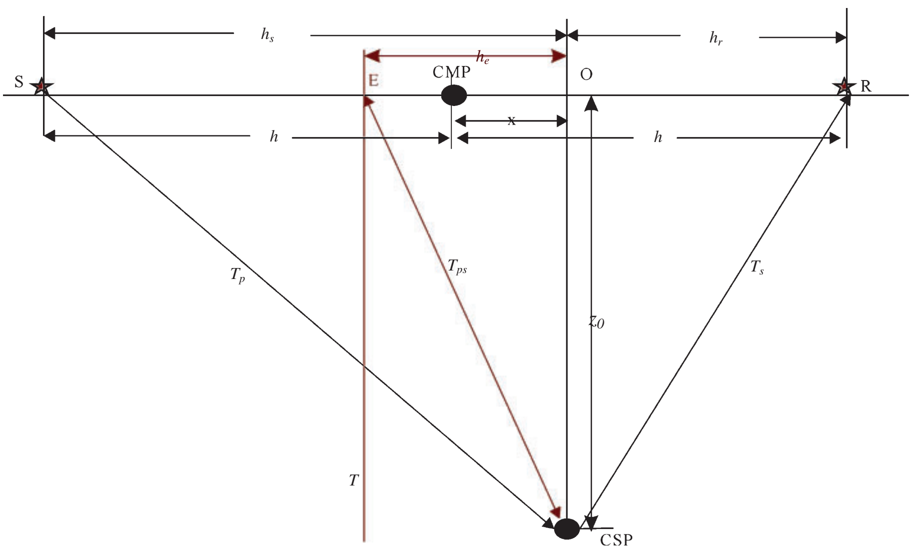

Fig. 1. Definition of the equivalent offset. S and R represent the source point and the receiver point, respectively. O is the surface location of the common scatter point (CSP), E is the equivalent point, Z_0 is the depth of the CSP, and x is the distance from the common mid-point (CMP) location to O; h is the half offset between S and R, h_e the equivalent offset, h_s the distance between S and O, and h_r the distance between R and O.

et al., 1994, 1998), *PS*-wave data can be migrated along with all other effectively scattered waves. Migration of CSP gathers can improve the SNR by increasing the stacking fold, and the method can be used to estimate the *PS*-wave velocity profile without using the *P*-wave velocity. In areas with complicated subsurface conditions, such as steep dips or laterally variable lithology, it is extremely difficult to obtain satisfactory imaging results with conventional CCP-gathers processing; the imaging method based on scattering waves can provide a better solution.

Bancroft et al. (1994) proposed the method of equivalent offset migration (EOM) and applied it to some *PS*-wave data

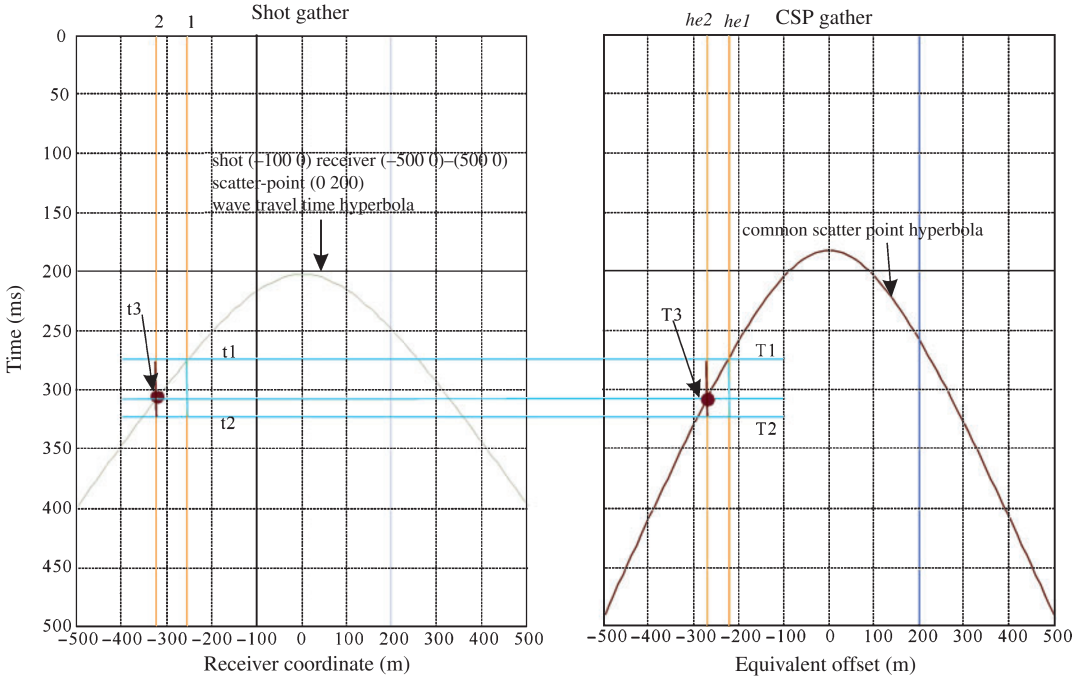

Fig. 2. Discretisation error due to the formation of a common scatter point (CSP) gather (right) from a common source gather (left).

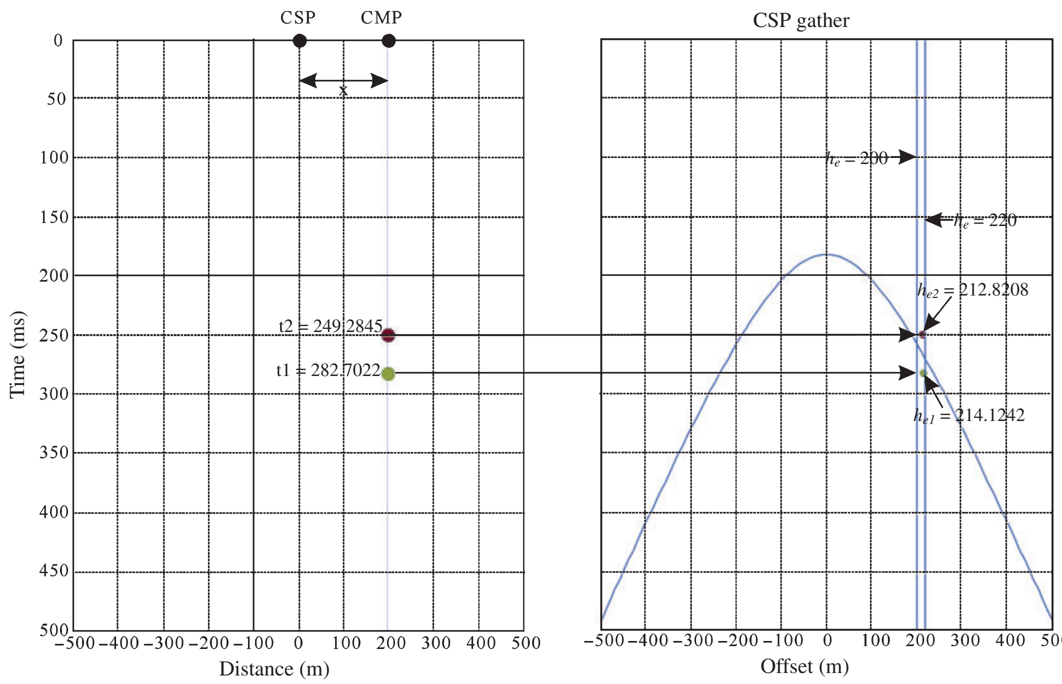

Fig. 3. Time shift, due to source and receiver co-location when a common scatter point (CSP) gather (right) is formed from input common mid-point (CMP) data (left). The scatter point is at (0 m, 200 m), the equivalent velocity is $2V_p/(1+r)$, in which the *P*-wave velocity (V_p) is 3000 m/s and the velocity ratio (r) is 1.732. The travel-time *t1* is the travel time when the source is at (100 m, 0 m) and receiver at (300 m, 0 m), *t2* is the travel-time after the source and receiver points co-located. The amplitudes at *t1* and *t2* are mapped into ($h_e = 200$, *t1*) and ($h_e = 200$, *t2*) on CSP gather, respectively, because of the spatial discretisation of equivalence offset. In theory, the positions are (h_{e1}, *t1*) and (h_{e2}, *t2*) on CSP gather.

(Bancroft and Wang, 1994). Here, we introduce some modifications of the EOM method to process 3-component seismic data without involving the *P*-wave velocity.

Basic theory

CSP gathers formation

Figure 1 describes how equivalent offset is defined (Bancroft et al., 1994). When the *P*-wave propagates from source S to the scatter point CSP and the converted *S*-wave propagates to receiver R, the total travel time is $T=T_p+T_s$ There exists a point E (the equivalent offset point) where, when the *P*-wave propagates from E to point CSP and the converted *S*-wave propagates back from CSP to E, the total travel time satisfies $T_{p+s}=T$. The following formula can be introduced (Bancroft and Wang, 1994):

$$\frac{(z_0^2+h_s^2)^{\frac{1}{2}}}{V_{pmig}}+\frac{(z_0^2+h_r^2)^{\frac{1}{2}}}{V_{smig}}=\frac{(z_0^2+h_e^2)^{\frac{1}{2}}}{V_{pmig}}+\frac{(z_0^2+h_e^2)^{\frac{1}{2}}}{V_{smig}} \tag{1}$$

where V_{pmig} and V_{smig} represent the *P*- and *S*-wave migration velocity, respectively.

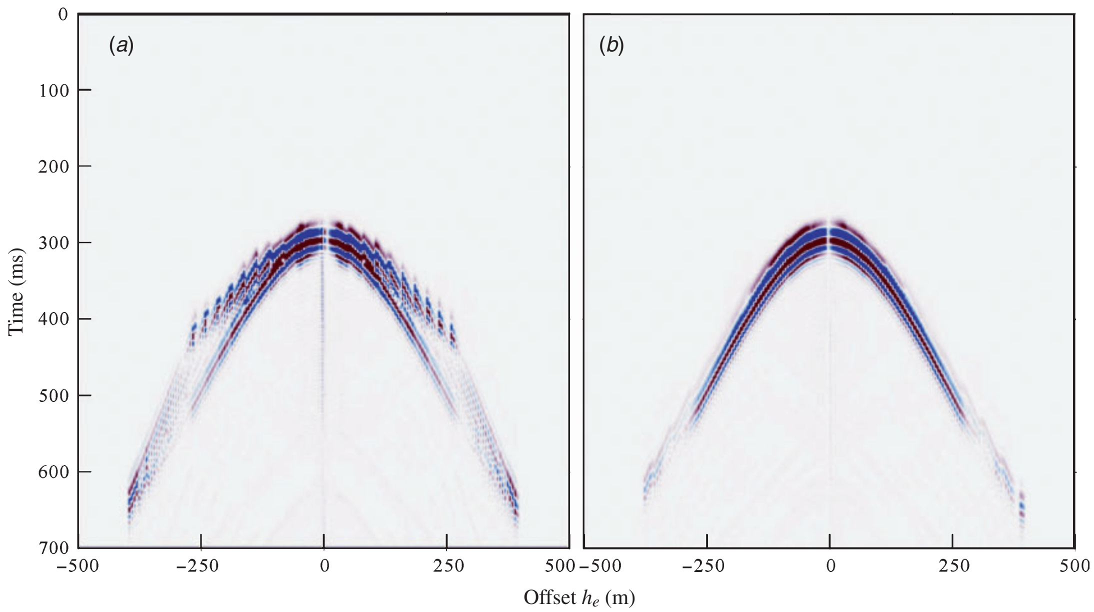

Fig. 4. Two common scatter point (CSP) gathers of *PS*-waves, in which (*a*) represents a CSP gather with step-shape divergent noise due to source and receiver co-location and (*b*) represents the CSP gather without source and receiver co-location.

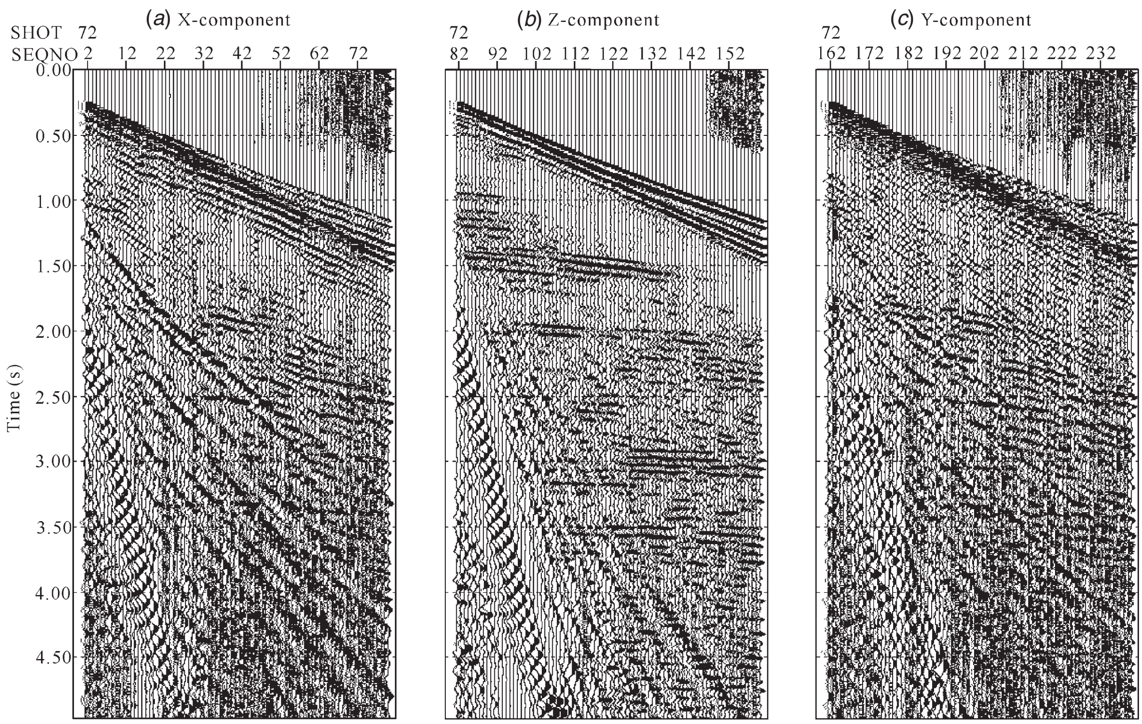

Fig. 5. A source gather of a 2D3C land seismic data.

Further it can be assumed that there is a class of seismic wave, which we call the equivalent *PS*-wave, that propagates from E to the scatter point CSP and back at the equivalent migration velocity V_{sem}. Then equation 1 can be rewritten as:

$$\frac{(z_0^2+h_e^2)^{\frac{1}{2}}}{V_{pmig}}+\frac{(z_0^2+h_e^2)^{\frac{1}{2}}}{V_{smig}}=\left[\left(\frac{2z_0}{V_{sem}}\right)^2+\left(\frac{2h_e}{V_{sem}}\right)^2\right]^{\frac{1}{2}}$$
$$=2\left[\left(\frac{T_0}{2}\right)^2+\left(\frac{h_e^2}{V_{sem}^2}\right)\right]^{\frac{1}{2}} \quad (2)$$

where $T_0=(1+\gamma_{mig})z_0/V_{pmig}$, $V_{sem}=(2V_{pmig}/1+\gamma_{mig})$, and γ_{mig} is the ratio of the *P*-wave to the *S*-wave migration velocity. It is obvious that the left side of equation 2 can be simplified as the equation of a hyperbola from the double square root equation.

Combining equations 1 and 2, the equation for constructing a CSP gather can be derived as

$$T=\frac{2\times h}{V_{sem}(x^2+h^2-h_e^2)^{\frac{1}{2}}}, \quad (3)$$

which means that the CSP gathers of the *PS*-wave are generated in a way similar to that of the common mid-point (CMP) gathers of the *P*-wave, the variables of which are defined in Figure 1. There are, however, two differences: one exists in the polarization of the converted *S*-wave, and the other is the equivalent *PS*-wave velocity.

Equation 3 differs from Bancroft's method (1994) since it does not need to calculate T_0 and avoids the transferred errors from the *P*-wave velocity estimation. In the generation of a CCP gather, only one trace from each relevant source is extracted. In the formation of a CSP gather, however, all traces within the migrated aperture can be used. This is why the EOM method can increase fold and improve SNR and imaging quality.

Optimisation

Discrete error

When the seismic data in a common-source gather are mapped into a CSP gather, they should not have any time shift. As illustrated in Figure 2, the time window [*t1*, *t2*] of traces 1 and 2 in the source gather corresponds to the time window [*T1*, *T2*] of traces He1 and He2 in the CSP gather and the amplitude at *t3* should be mapped into a scattering hyperbola in the corresponding CSP gather. However, the discrete equivalent offset error may cause *T3* in the CSP gather, which corresponds to time *t3* in the source gather, deviating from the scattering hyperbola. This discrete error may occur for both *P*- and *PS*-waves (Yin, 2005, 2009) and can be reduced by decreasing the equivalent offset interval in a CSP gather.

Error from co-location of source and receiver points

A problem in generating CSP gathers from source records is that the velocity difference in the incident and scattered path will cause a travel time difference when the points of source and receiver are co-located, and the travel time difference will increase with offset. As shown in Figure 3, when source and receiver locations are reciprocal, the travel time *t1* of the *PS*-wave becomes *t2*, where *t1* is the travel time for a source located at 100 m and a receiver located at 300 m, and *t2* is the travel time for a source located at 300 m and a receiver located at 100 m. When the *PS*-wave CSP gather is formed with equation 3 and equivalent velocity V_{sem}, *t1* and *t2* are mapped to *T1* and *T2*, respectively, and *T2* deviates from the scattering hyperbola.

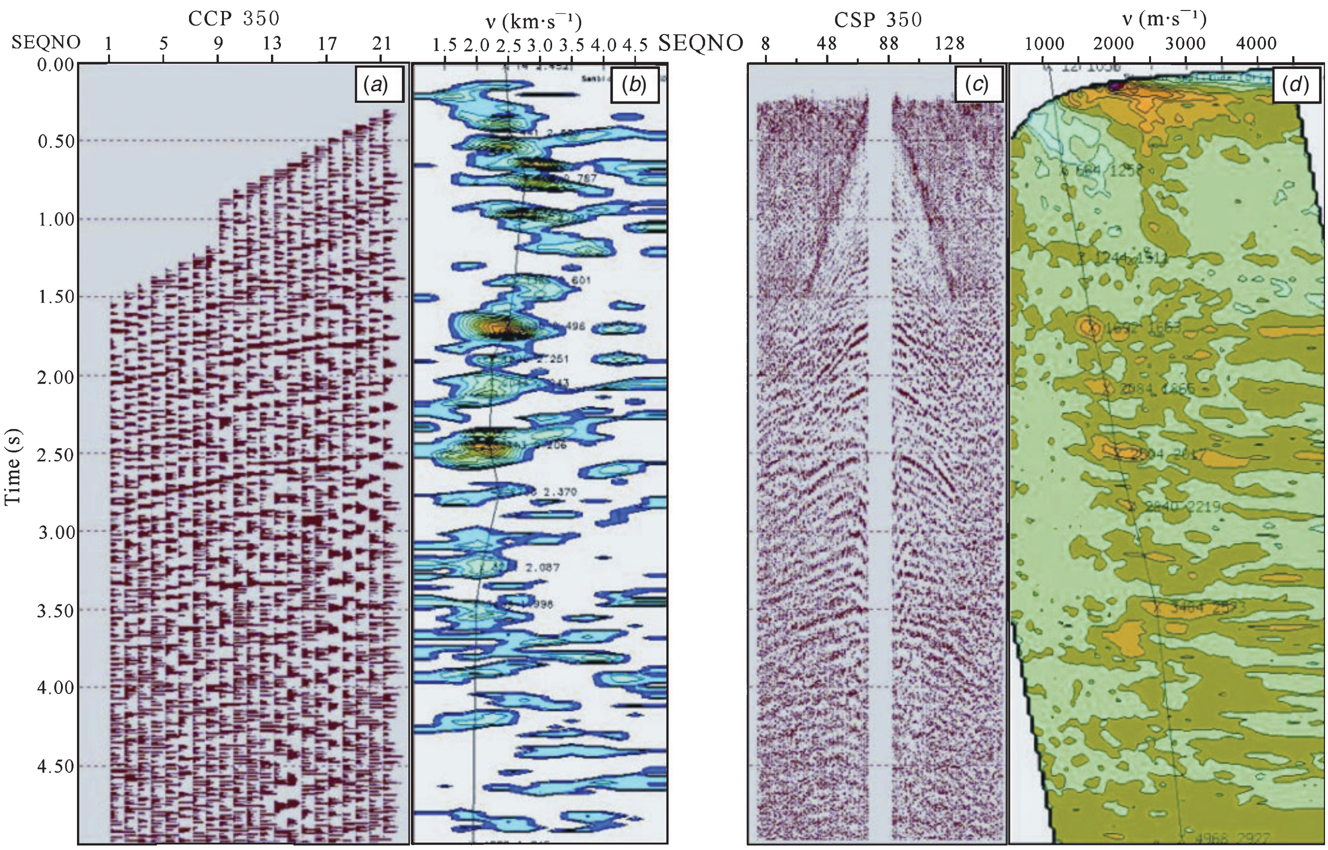

Fig. 6. Comparison of the (*a*) common conversion point (CCP) and (*c*) common scatter point (CSP) gathers in velocity analysis. (*b*) is the stacked velocity spectrum of (*a*), and (*d*) is the stacked velocity spectrum of (*c*).

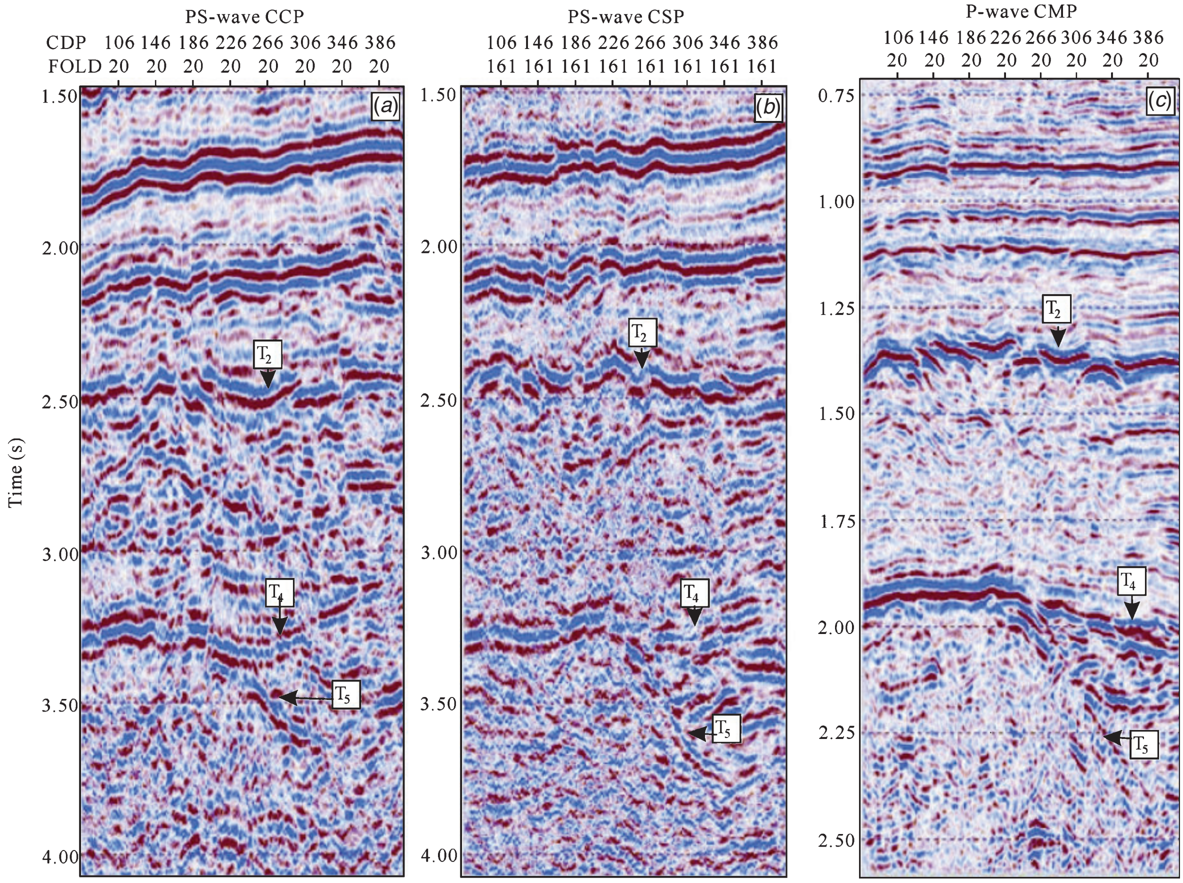

Fig. 7. Comparison of migrated time sections. (*a*) is the migrated section based on common conversion point (CCP) gathers, (*b*) is based on common scatter point (CSP) gathers, and (*c*) is the post-stack time migrated *P*-wave section. In this figure, T2 represents reflections from Cenozoic sandstone, T4 represents reflections from the top of the igneous reservoir and T5 represents reflections from the bottom of the igneous reservoir.

It can be inferred that the time difference $\Delta t = T2\text{-}T1$ will increase with offset, and the scattering hyperbola diverges into a step-shape (Figure 4*a*). Since the divergent noise has a negative effect on migration, it has to be suppressed. However, if source and receiver points are not co-located, the divergent energy can be very small (Figure 4*b*).

Field data analysis

To demonstrate the method, we applied it to a 2 dimensional 3-component (2D3C) field seismic dataset acquired in the Songliao Basin in North Eastern China. The X-, Y- and Z-components of a source record are shown in Figure 5. The data were sampled to identify an igneous reservoir where conventional *P*-wave imaging is not adequate to describe the reservoir. Only weak reflections are received from the inner igneous reservoir so it is not possible to image clearly, since there is a strong impedance difference between igneous and sedimentary formations. Methods based on CCP gathers and on the CSP gathers are applied for comparison. The *P*-wave data were processed in the conventional way. The CCP and CSP gathers of the *PS*-waves are shown in Figure 6*a* and 6*c*. Figure 6*b* and 6*d* are the velocity spectra of the CCP and CSP gather, respectively. They reveal that the CSP gather has a higher SNR than the CCP gather, especially in the target reflection zone of [3.0 s, 4.0 s]. There are 161 traces in the CSP gather, while there are only 20 traces in the CCP gather, and this causes the SNR difference.

Figure 7*a* and 7*b* are migrated time sections from the CCP method and the CSP methods, respectively. Figure 7*c* is the post-stack migration of the *P*-wave data. In Figure 7*b*, the image quality between horizons T2 to T4 is better than that of Figure 7*a*. For the volcanic reservoir imaging, Figure 7*b* shows better details of the igneous body (between T4 and T5) and the unconformity contact (T5).

Conclusions

Based on the *PS*-wave EOM method (Bancroft et al. 1994), an equivalent *PS*-wave velocity in the ray path between the equivalent offset point and scatter point was assumed, and the EOM method has been simplified to migrate *PS*-wave data without using the *P*-wave velocity. Moreover, the modified method can suppress significantly the step-shaped divergent noise. The results of a real 2D3C data analysis show that the image quality with the modified EOM is better than that based on the CCP gathers.

Acknowledgements

The authors acknowledge the funding of the China Natural Science Foundation (No.40574055), National 973 Program (No. 2006CB202207) and National Key Sci. & Tech. Program (No. 2011ZX05: 035–001–006HZ, 035–002–003HZ, 008–006–22, 049–01–02, and 019–003). Dr G. M. Yu is thanked for helping pre-processing the field *P*- and *PS*-wave data, and David Booth and Dr Z. P. Qian are also thanked for improving the English writing of this paper.

References

Aki, K., and Richards, P., 1980, *Quantitative seismology, Vol. 2*: W. H. Freeman.

Bancroft, J. C., and Wang S., 1994, Converted-wave prestack migration and velocity analysis by equivalent offsets and CCP gathers. CREWES Research Report, 6: 28.1–28.7.

Bancroft, J. C., Geiger, H. D., Foltinek, D., and Wang, S., 1994, Prestack migration by equivalent offsets and CSP gathers. CREWES Report, 6: 27.1–27.18.

Bancroft, J. C., Geiger, H. D., and Margrave, G. F., 1998, The equivalent offset method of prestack time migration: *Geophysics*, **63**, 2042–2053. doi:10.1190/1.1444497

Wu, R. S., and Aki, K., 1985, Scattering characteristics of elastic waves by an elastic heterogeneity: *Geophysics*, **50**, 582–595. doi:10.1190/1.1441934

Yin, J. J., 2005, Study of numerical simulation of seismic scatter wave [D]. China University of GeoSciences, Beijing, China, 80–86.

Yin, J. J., 2009, The scattered wave imaging method [Research Report]. Institute of Geology & Geophysics, China Academy of Sciences (CAS), Beijing, China, 48–49.